BL8B2
Electronic Structure at Highly Ordered Organic/Metal Interfaces

H. Yamane[*], K. Kanai, K. Seki

Department of Chemistry, Nagoya University, Nagoya 464-8602, Japan

The electronic structure at the interface formed between an organic semiconductor film and a metal electrode plays a crucial role in the performance of electronic devices using organic semiconductors such as electroluminescent displays, field-effect transistors, and photovoltaic cells. In particular, the energetics of the molecular energy levels near the Fermi level (E_F) of metals, *i.e.*, the energy level alignment at organic/metal interfaces, are of fundamental importance in discussing various charge phenomena related to organic devices such as the barrier heights for the charge injection and separation at the interface [1]. In the field of organic/metal interfaces, one of the important issues is the elucidation and control of the *interface state*, which may dominate the energy level alignment at organic/metal interfaces. However, it is generally not easy to discuss the interfacial electronic structure precisely since the energetics at organic/metal interfaces is easily modified by the presence of the interface-specific electrical and geometrical phenomena. To fully clarify the possibly complicated electrical and geometrical phenomena at the interface, a more pertinent experimental approach to this issue would be to use a well-characterized system, *e.g.*, epitaxially grown organic thin film on atomically flat and clean metal single crystal surfaces, in quantitative electron spectroscopic measurements.

From the above point of view, by using angle-resolved UV photoemission spectroscopy (ARUPS), we have studied the electronic structure of well-ordered thin films of metal-phthalocyanines (M-Pc), perylene-tetracarboxylic dianhydride (PTCDA), and pentacene (Pn) prepared on metal single crystal surfaces. Among these, it was reported that Pn molecules on Cu(110) in the monolayer regime form a highly ordered film structure with planar adsorption geometry, where the molecular long axis is parallel to the [1$\bar{1}$0] substrate direction [2].

Figure 1(a) and (b) shows the observed energy versus momentum [$E(k_{\parallel})$] relation for the flat-lying Pn monolayer film on Cu(110) along (a) $\phi = 0°$ (the [1$\bar{1}$0] substrate direction) and (b) $\phi = 28°$. The abscissa is the parallel momentum component ($k_{\parallel}$), and ordinate is the binding energy (E_b) relative to the E_F of the substrate. In order to map out the $E(k_{\parallel})$ relation, we took the second derivative of the raw ARUPS spectra [$-d^2I(E_b)/dE_b^2$] at $hv = 20$ eV after smoothing for specifying the energies of the spectral features. Open and filled circles indicate the peak position of the Pn-derived peaks A–C in the raw ARUPS spectra measured at $hv = 20$ and 30 eV, respectively. The selected raw ARUPS spectra of the

valence levels and the secondary-electron cutoff are shown in Fig. 1(c) and (d), respectively. We found that (i) the change in the work function (*i.e.*, vacuum level shift Δ) upon the adsorption of the flat-lying Pn monolayer film is $\Delta = -0.9$ eV [Fig. 1(d)] due to the formation of the interfacial dipole layer [1], and that (ii) peaks A–C are the interface-specific states. The latter finding (ii) was concluded since the energy positions and the orbital symmetries of peaks A–C cannot be explained by the UPS spectrum of the gas-phase Pn [3] and its orbital symmetries [4]. These interface states A–C may originate from the molecular energy levels split due to the hybridization with the wave function of the substrate, which can modify the energies and the orbital symmetries, as in the case of the Pn/Cu(119) interface reported by Ferretti *et al* [5]. According to their theoretical calculation in Ref 5 based on the density-functional theory, the density-of-states just below E_F and peak A in Fig. 1 can be ascribed to the resultant split levels of the former lowest unoccupied molecular orbital (LUMO) level, and peaks B and C in Fig. 1 can be ascribed to the resultant split levels of the former highest occupied molecular orbital (HOMO) level.
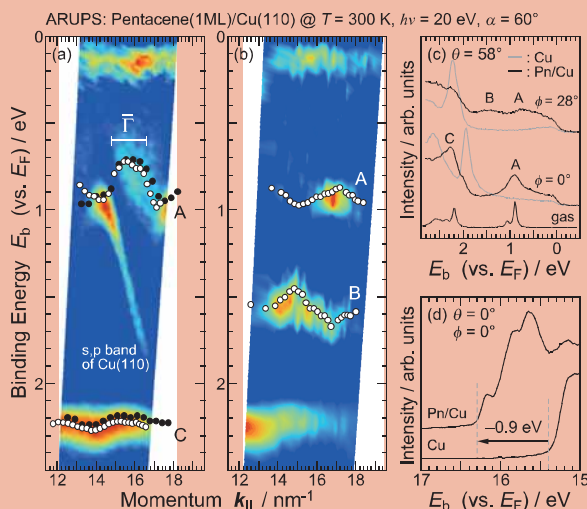

Fig. 1. (a,b) $E(k_{\parallel})$ relation for the highly ordered flat-lying Pn monolayer film on Cu(110) at $\phi =$ (a) 0° and (b) 28°. The abscissa is the parallel component of the momentum ($k_{\parallel}$), and ordinate is the binding energy (E_b) relative to the Fermi level (E_F) of the substrate. Open and filled circles indicate the position of the Pn-derived peaks measured at $hv = 20$ and 30 eV, respectively. (c,d) Selected ARUPS spectra of the Pn monolayer film and the bare substrate for the regions of (c) valence levels and (d) secondary-electron cutoff.

It is interesting to note that, as seen in Fig. 1(a) and (b), the interface states A–C show dispersive behavior. At $\phi = 0°$ [Fig. 1(a)], the $E(k_\|)$ curve of peak A measured at $h\nu = 20$ eV corresponds well with that measured at $h\nu = 30$ eV, and the $E(k_\|)$ curve of peak C has turning points at the same $k_\|$ as that for peak A. At $\phi = 28°$ [Fig. 1(b)], the turning points for peak B appears at the same $k_\|$ as that for peak A, and the phase of the $E(k_\|)$ curve for peak B is opposite to that for peak A. Furthermore, the experimentally observed $\bar{\Gamma}$ point ($\bar{\Gamma}_{exp}$) exists around $k_\| = 15.7\pm0.9$ nm^{-1} at $\phi = 0°$, which is the center of the fifth Brillouin zone. From the $E(k_\|)$ curves of peaks A and C, we can estimate the lattice constant (λ) along the $[1\bar{1}0]$ substrate direction using the relation $\lambda = 2\pi/K$, where K is the size of the Brillouin zone, under the assumption of a tight-binding model. The deduced value of λ is 1.6 nm, which agrees well with the lattice constant of the flat-lying Pn monolayer film along the $[1\bar{1}0]$ substrate direction [2]. Thus, the observed dispersive behavior can be ascribed to the intermolecular band dispersion in the flat-lying Pn monolayer film on Cu(110) with a large bandwidth of 0.25 eV for the uppermost valence band A, which seems to form a free-electron-like parabolic dispersion. Thus, the effective mass of the hole (m_h^*) can be calculated from

$$\frac{1}{m_h^*} = \frac{1}{\hbar^2}\frac{\mathrm{d}^2 E(k)}{\mathrm{d}k^2}.$$

Using this equation, we estimated m_h^* to be $0.24m_0$ at 300 K within the tight-binding approximation. In the case of usual π-conjugated flat-lying organic monolayers, the intermolecular interaction is mainly dominated by the weak intermolecular σ-σ interaction, which gives small bandwidth of less than 0.05 eV. The observed band dispersion with rather small m_h^* may originate from the intermolecular interaction *via* the substrate due to the hybridization between the molecular orbitals and the free-electron-like Cu bands. On the other hand, Temirov *et al.* reported the inplane intermolecular band dispersion for the unoccupied state in a PTCDA monolayer on Ag(111) with an effective mass of electron m_e^* of $0.47m_0$ by using the high-resolution scanning tunneling microscopy and spectroscopy [6]. The observed dispersion in Ref 6 is far larger than expected for the PTCDA monolayer alone [7], and they suggest that the dispersion might be related to the surface state since the effective mass is similar to that of the Ag(111) surface. However, in the case of pentacene/Cu(110), there is no known surface state along the $[1\bar{1}0]$ substrate direction on the Cu(110) surface within the observed energy window. It must therefore be concluded that the mechanisms of interfacial dispersion of π-conjugated molecules are not yet fully understood. For further consideration about this issue, a joint experimental and theoretical study is now in progress.
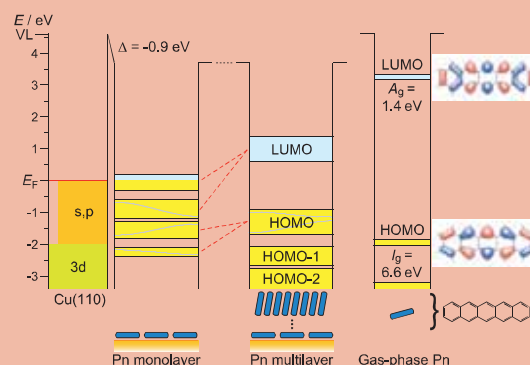

Fig. 2. Energy level diagrams for the Pn/Cu(110) system and the gas phase Pn. The LUMO energy for the Pn multilayer was estimated from Ref 8. The ionization energy for gas phase Pn (I_g) is 6.6 eV [3], and the intermolecular polarization energy for holes can be estimated to be 1.7 eV. If the intermolecular polarization energy for electrons is equal to that for holes, the electron affinity for gas phase Pn (A_g) can be estimated to be 1.4 eV.

In summary, the energy level diagram for the Pn/Cu(110) system is presented in Fig. 2. From the UPS spectra in Fig. 1, the work function of the clean Cu(110) surface is 4.6 eV and its change (Δ) by the Pn adsorption is −0.9 eV. For the flat-lying monolayer film, we clearly observed the electronic structure characteristic of the interface with the following findings: (i) formation of the interface states with possible modification of the orbital symmetry and the energy position, and (ii) two-dimensional inter-molecular band dispersion of these interface states with m_h^* for the upper branch being 0.24 m_0 at 300 K. These interface states can be deduced to originate from the hybridization of the molecular orbitals such as the HOMO and the LUMO levels with the wave function of the substrate, which may also lead to the observed band dispersion by the intermolecular interaction through the substrate. Further studies on the correlation between the electronic and the film structures would lead to a breakthrough for the understanding of charge phenomena in organic solids.

*Present address: Institute for Molecular Science
E-mail: yamane@ims.ac.jp

[1] H. Ishii *et al.*, Adv. Mater **11** (1999) 605.
[2] S. Lukas *et al.*, Phys. Rev. Lett. **88** (2001) 028301; S. Söhnchen *et al.*, J. Chem. Phys. **121** (2004) 525.
[3] V. Coropceanu *et al.*, Phys. Rev. Lett. **89** (2002) 275503.
[4] H. Yamane *et al.*, Phys. Rev. B, **76** (2007) 165436; Phys. Stat. Sol. (b), **245** (2008) 793.
[5] A. Ferretti *et al.*, Phys. Rev. Lett., **99** (2007) 046802.
[6] R. Temirov *et al.*, Nature, **444** (2006) 350.
[7] H. Yamane *et al.*, Phys. Rev. B, **68** (2003) 033102.
[8] F. Amy *et al.*, Org. Electron. **6** (2005) 85.

Synchrotron Radiation Stimulated Etching of Polydimethylsiloxane with XeF$_2$

T.Y. Chiang[1], T. Makimura[2], C. S. Wang[3], T. Urisu[1,4]

[1]Institute for Molecular Science, Okazaki 444-8585 Japan
[2]Tsukuba University, 1-1-1Tennoudai Tsukuba, Ibaraki 305-8573 Japan
[3]Shanghai Jiao Tong University, 1954 Hua Shan Rd. Shanghai 200030 P. R. China
[4]The Groduate University for Advanced Studies, Okazaki 444-8585 Japan

The synchrotron radiation (SR) stimulated etching of silicon elastomer polydimethylsiloxane (PDMS) has been demonstrated with XeF$_2$ as the etching gas. An etching system with a differential pump and paraboloid mirror was constructed to perform the etching. The PDMS was found to be effectively etched under the SR irradiation with flowing XeF$_2$, and the etching process was area-selective and anisotropic. An etching rate of about 45μm・150mA^{-1}・min^{-1} was obtained at a XeF$_2$ atmosphere of 0.5 Torr in etching chamber.
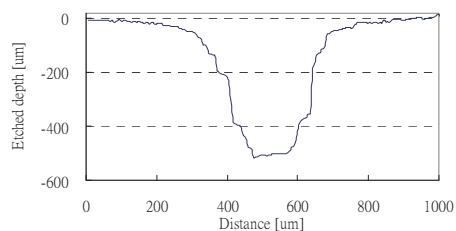

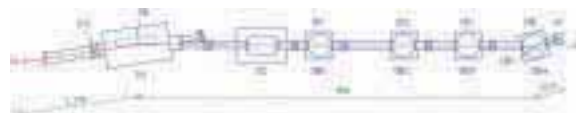Fig. 4. Depth profile of the etched pattern shown in Fig. 3.

Fig. 1. Schematic view of the beam line 4 A. DP$_i$: differential pumpimg chamber. TMP: turbo molecular pump, IP: ion pump, EC: etching chamber. FM: focusing mirror.
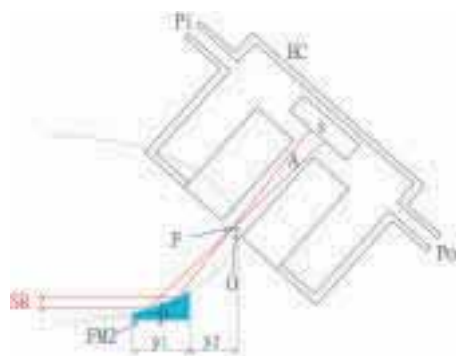

Fig. 2. Beam trace in focusing mirror chamber and etching chamber. S: specimen, A: aperture EC: etching chamber FM: focusing mirror.
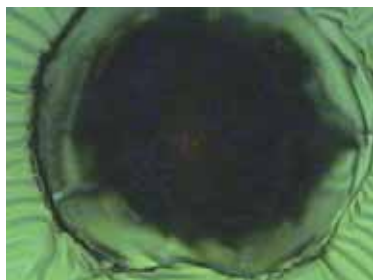

Fig. 3. Top view of the etched pattern on PDMS by SR etching using XeF$_2$ gas.

135

Characterization of Self-Assembled Co Nanorods Grown on Cu(001)-(2×3)N Studied by XMCD

X. D. Ma[1, 2], T. Nakagawa[1, 3], Y. Takagi[1, 3], M. Przybylski[2], J. Kirschner[2], T. Yokoyama[1,3]

[1]*Department of Structural Molecular Science, The Graduate University for Advanced Studies (Sokendai), Myodaiji-cho, Okazaki, Aichi 444-8585, Japan*
[2]*Max-Planck-Institut für Mikrostrukturphysik, Weinberg 2, 06120 Halle, Germany*
[3]*Institute for Molecular Science, Myodaiji-cho, Okazaki, Aichi 444-8585, Japan*

Introduction

Recently, York and Leibsle [1] discovered self-assembled growth of well extended Co nanorods on Cu(110)-(2×3)N. The Co nanorods are well isolated from each other up to as much as ~2.0 monolayer (ML) Co coverage with six times intervals along the [001] direction. We have here investigated XMCD of 0.8 ML Co/Cu(110)-(2×3)N substrates.

Experimental

A Cu(110) single crystal was dosed with N by mild N_2^+ bombardment and subsequent annealing at ~473 K to yield (2×3)N surfaces. Co was deposited on these surfaces at ambient temperature using a commercial evaporator. The angle-dependent Co L-edge XMCD measurements were performed with a total electron yield mode using a UHV-compatible superconducting magnet (7 T) XMCD system with a liq. He cryostat (the sample temperature of 4.9 K).

Results and Discussion

Figure 1 depicts the magnetization curves recorded with the electron yield at the L_{III} peak top energy. The magnetizations are found to be almost saturated at $H=\pm5$ T for all the axes ([001] is the easy axis). The curves were simulated using a simple second-order magnetic anisotropy model to deduce the macroscopic magnetic anisotropy constants. The two magnetic anisotropy constants K_P and K_A respectively caused by the planar (film origin) and axial (rod origin) anisotropies and the size of the spin block N were assumed. The parameters were determined as $K_P=1.2\times10^{-4}$ (eV/atom), $K_A=2.0\times10^{-5}$ (eV/atom), and $N=15$ (atom). The planar magnetic anisotropy K_P that makes the surface normal the hardest axis is found to be much larger than that of the rod axial anisotropy K_A.

The angle dependence of the XMCD spectra shown in Fig. 2 was analyzed. The results are $m^x_{orb}=0.23$ μ_B, $m^y_{orb}=0.19$ μ_B, $m^z_{orb}=0.16$ μ_B, $m^x_T=-0.005$ μ_B, $m^y_T=0.011$ μ_B, $m^z_T=-0.006$ μ_B, and $m_{spin}=1.01$ μ_B, where m_T is the magnetic dipole moment. The orbital magnetic moment decreases in the sequence of x ([001]), y ([1-10]), and z ([110]), which is consistent with the above magnetic anisotropy constants. This consequently implies that the magnetic anisotropy originates from the difference in the spin-orbit interaction. Note that the spin magnetic moment obtained is significantly smaller than that of the bulk *hcp* Co,

because the small spin magnetic moment in Co may originate from the strong covalent bonds with N in the present nanorods.
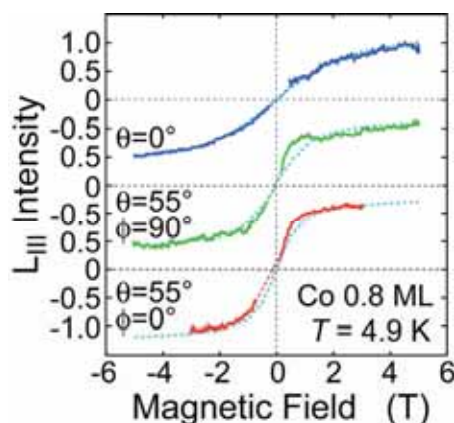

Fig. 1. Magnetization curves at T=4.9 K recorded with the intensity at the L_{III} peak energy. The simulated magnetization curves using a simple magnetic anisotropy model are also shown.
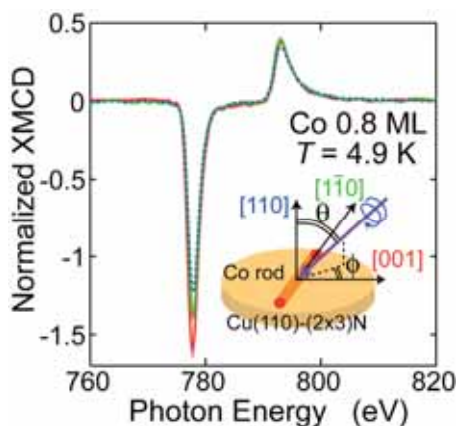

Fig. 2. Co L-edge XMCD spectra of 0.8 ML Co on Cu(110)-(2×3)N at T=4.9 K and $H=\pm5.0$ T for $\theta_{in}=0°$ (blue) and $(\theta_{in},\varphi_{in})=(55°,90°)$ (green) and $H=\pm3.0$ T for $(\theta_{in},\varphi_{in})=(55°,0°)$ (red).

[1] S. M. York, F. M. Leibsle, Phys. Rev. B **64** (2001) 033411.

Enhancements of Spin and Orbital Magnetic Moments of Submonolayer Co on Cu(001) Studied by XMCD

T. Nakagawa[1], Y. Takagi[1], T. Yokoyama[1]

[1]*Institute for Molecular Science, Okazaki 444-8585, Japan*

Introduction

Enhancements of the magnetic moments of ultra-thin films have extensively been investigated both theoretically and experimentally because of their importance in fundamental physics as well as techno-logical applications to magnetic recording media. In the present work, we have investigated the enhance-ments of spin and orbital magnetic moments for sub-monolayer Co/Cu(001) by means of XMCD using a UHV-compatible XMCD system with a 7 T super-conducting magnet and a liquid He cryostat [1].

Experimental

A submonolayer Co film was deposited on a clean Cu(001) surface from a commercial evaporator. The thickness of the film investigated was estimated to be 0.4 ML from the Co L-edge absorption intensity. Co $L_{III,II}$-edge circularly polarized X-ray absorption spectra were recorded at the X-ray incidence polar angles θ_{in} of 60° (grazing incidence) and 0° (normal incidence). The spectra were taken at 6.0 K by switching the magnetic field.

Results and Discussion

Figure 1 shows the magnetization curve of 0.4 ML Co at 6.0 K along the surface normal [001] direction, which is the magnetically hardest axis. The data were scaled using the area of the Co L_{III} peak. The XMCD intensity is found to increase linearly up to $H=\pm2.5$ T, while the values at $H=\pm5.0$ T are apparently weaker than the ones expected from the extrapolated linear line. By fitting the experimentally obtained data points with a second-order magnetic anisotropy model, the lowest magnetic field for saturation is estimated to be ~3.4 T. The magnetic fields of ±5 T are thus confirmed to saturate the magnetization even along the magnetically hardest [001] axis.

Figure 2 depicts the Co $L_{III,II}$-edge XMCD spectra for $\theta_M=90°$ and 0°, where θ_M denotes the polar angle of magnetization. Although the two XMCD spectra are not very different from each other, small dissimilarities can clearly be seen around the $L_{III,II}$-edge peaks, indicating small anisotropic features in the present submonolayer film.

Using the sum rules and the formulas of XMCD angle dependence, the magnetic dipole terms were obtained to be $m_T^{//}=0.010\pm0.05$ μ_B and $m_T^{\perp}=-0.020\pm0.05$ μ_B. Consequently, the spin magnetic moment was given as 1.79 ± 0.10 μ_B, which is larger than that of bulk *hcp* Co (1.55 μ_B), and the orbital magnetic moments of $m_{orb}^{//}=0.29\pm0.05$ μ_B and $m_{orb}^{\perp}=0.23\pm0.05$ μ_B are much more significantly greater than the bulk value of 0.15 μ_B. Theoretical estimations for the spin and orbital magnetic moment of monolayer Co/Cu(001) were reported as $m_{spin}=1.85$ μ_B and $m_{orb}=0.261$ μ_B [2], which are consistent with the present results. Enhancements of the magnetic moments compared with the corresponding bulk values were thus clearly elucidated: ~12% for the spin magnetic moment and ~96 and ~53% for the orbital magnetic moments along the surface parallel and normal directions, respectively.
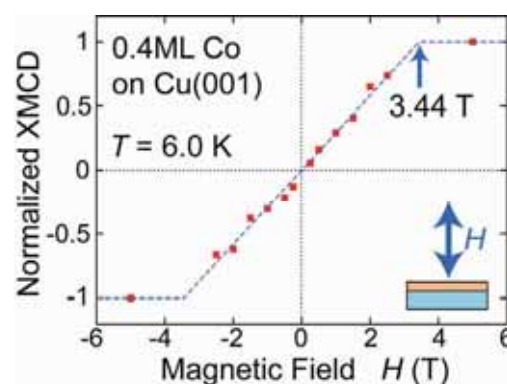

Fig. 1. Magnetization curve of 0.4 ML Co/Cu(001) at 6.0 K along the [001] direction, recorded as a normalized Co L_{III} XMCD intensity. The red points are the experimental data, and the blue dashed line is the fitted result.
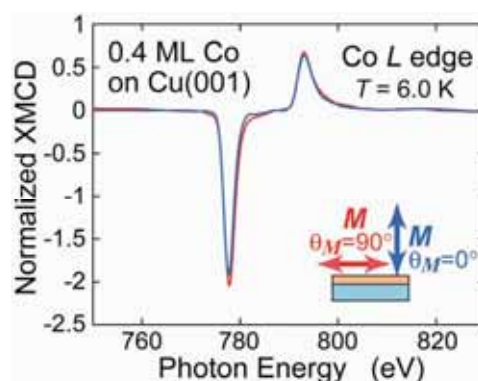

Fig. 2. Co $L_{III,II}$-edge XMCD spectra of 0.4 ML Co on Cu(001) at 6.0 K for the magnetization parallel ($\theta_M=90°$) and perpendicular ($\theta_M=0°$) to the surface.

[1] T. Nakagawa, Y. Takagi, Y. Matsumoto, T. Yokoyama, this volume & also Jpn. J. Appl. Phys., *in press*.
[2] O. Hjortstam, J. Trygg, J. M. Wills, B. Johansson, O. Eriksson, Phys. Rev. B **53** (1996) 9204.

Variation of Magnetic Anisotropy upon Adsorption of NO on Co/Cu(001) Studied by XMCD

T. Nakagawa[1], Y. Takagi[1], T. Yokoyama[1]

[1]*Institute for Molecular Science, Okazaki 444-8585, Japan*

Introduction

Adsorption of atoms and molecules on magnetic thin films is an attractive surface scientific subject since it .is known to change drastically magnetic anisotropy and to induce sometimes spin reorientation transitions. In the present work, we have investigated NO adsorption on submonolayer Co/Cu(001) by means of XMCD using a UHV-compatible XMCD system with a 7 T super- conducting magnet and a liquid He cryostat [1].

Experimental

A 0.8 monolayer (ML) Co film was deposited on a clean Cu(001) surface from a commercial evaporator at room temperature and was subsequently dosed with NO at ~100 K. Co $L_{III,II}$-edge circularly polarized X-ray absorption spectra were recorded at T=5.0 K and H=5.0 T with the X-ray incidence polar angles θ_{in} of 55° (grazing incidence) and 0° (normal incidence).

Results and Discussion

Figure 1 depicts the magnetization curves of 0.8 ML Co on Cu(001), recorded as Co L_{III} XMCD intensity at the peak top energy. Unfortunately, the curve along the hard axis of θ_{in}=0° is not saturated. Using the θ_{in}=0° data, the second-order magnetic anisotropy constants including demagnetization energies are obtained as K_2=−370 (μeV/atom) for clean Co and −130 (μeV/atom) for NO adsorbed Co. This indicates significant suppression of the in-plane magnetic anisotropy upon NO adsorption.

Figure 2 depicts the Co $L_{III,II}$-edge XMCD spectra for θ_{in}=55° and 0°. NO adsorption induces the shift of the peak energies and the suppression of the XMCD intensity. Using the sum rules, the spin and orbital magnetic moments are derived. Although the magnetization for clean Co (θ_{in}=0°) is not saturated, the ratio m_{orb}/m_{spin} was assumed to be invariant to yield the orbital magnetic moment. In the case of NO adsorption, both the magnetizations were assumed to be saturated and this allows us to evaluate magnetic dipole terms appropriately and hence the intrinsic spin magnetic moments.

The d-hole number is found to increase significantly from d_h=2.56±0.13 (clean) to 2.92±0.15 (NO-ads.), implying the oxidation of Co upon NO adsorption. The spin magnetic moment noticeably decreases from m_{spin}=1.780±0.18 μB (clean) to 0.89 ±0.05 μB (NO-ads.). This indicates strong interaction between an unpaired electron of NO and exchange-split Co 3d levels. The anisotropic orbital magnetic moments show the most prominent difference. For clean Co, the analysis yields $m_{orb}^{//}$=0.299±0.02 μB and $m_{orb}^{\perp}$=0.228±0.02 μB, while the NO-adsorbed Co gives $m_{orb}^{//}$=0.106±0.01 μB and $m_{orb}^{\perp}$=0.111±0.01 μB. These results clarifies that the strong in-plane magnetic anisotropy in clean Co is derived from much larger in-plane spin-orbit interaction than the perpendicular one and that NO adsorption leads to the loss of anisotropy in the spin-orbit interaction. The weak in-plane magnetic anisotropy for NO adsorbed Co may originate from the demagnetization energy (shape anisotropy).
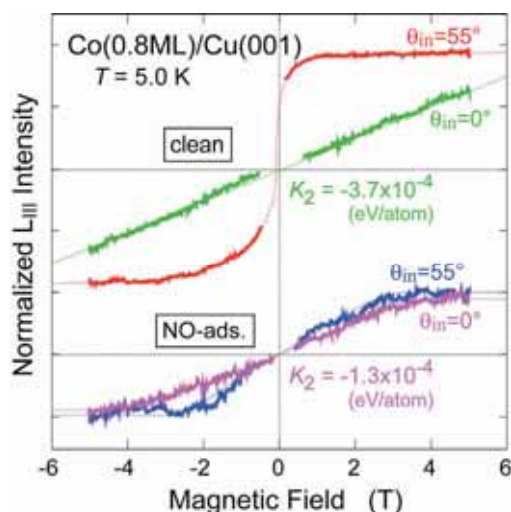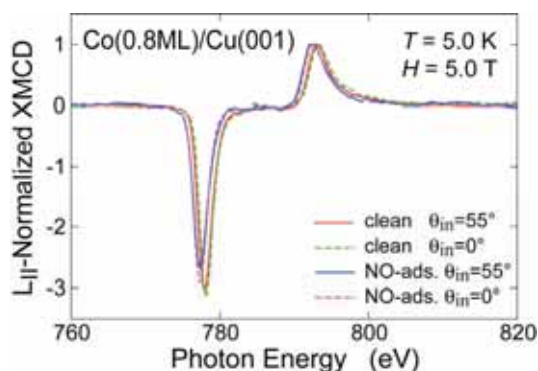

Fig. 1. Magnetization curves of 0.8 ML Co on Cu(001) at T=5.0 K before and after NO adsorption.

Fig. 2. Angle dependent Co $L_{III,II}$-edge XMCD spec-

tra of 0.8 ML Co on Cu(001) at T=5.0 K before and after NO adsorption.

[1] T. Nakagawa, Y. Takagi, Y. Matsumoto, T. Yokoyama, this volume & also Jpn. J. Appl. Phys., *in press*.

Photoelectron Angular Distribution of Mn-Phthalocyanine Monolayer on Ag(111)

T. Aoki[1], S. Hosoumi[1], C. Karino[1], R. Sumii[2], S. Nagamatsu[1], N. Ueno[1], S. Kera[1]

[1]Graduate School of Advanced Integration Science, Chiba University, Chiba 263-8522 Japan
[2]Graduate School of Science, Nagoya University, Nagoya 464-8602 Japan

Origins of the energy position and the shape of HOMO bands are keys to understand interface properties of organic films. The electronic structure of the adsorbed monolayer on a metal substrate is generally modified much by a strong electronic coupling. In this study changes in the electronic structure due to different spin configuration and/or change in the ligand field upon adsorption were investigated for Mn-phthalocyanene (MnPc) on Ag(111). Angle-resolved UPS (ARUPS) using synchrotron radiation is a powerful tool to study the geometrical structure of the ultrathin films of organic molecules as well as the electronic structure. In the previous work we have succeeded to analyze the emission (θ) and azimuthal (ϕ) angle dependences of ARUPS of thin films of large organic molecules using single scattering approximations [1].

In this report, we show the observed θ and ϕ dependences of 2p- and 3d-orbital derived bands in ARUPS spectra for well-ordered MnPc monolayer (ML) on the Ag(111) substrate.

Experimental

θ and ϕ dependences of ARUPS spectra were recorded at photon incidence angle $\alpha=45^{\circ}$, hν=28 eV, and T=295 K. The purified MnPc molecules were carefully evaporated onto a clean Ag(111) substrate. We confirmed 6-hold molecular domains (2 domains in each crystal axis) from LEED results.

Results and Discussion

Figure 1 shows a typical HeI UPS spectrum of annealed-MnPc (ML)/Ag(111) at θ =0°. The results obtained for MnPc (ML) /HOPG are also shown [2]. For MnPc/Ag(111), feature A appearing at 0.35 eV, which is located at lower energy position than MnPc/HOPG, can be ascribed to HOMO band of MnPc. Feature B, HOMO-1, which is located at similar energy position as for MnPc/HOPG, might be assigned to a single π MO as observed in other various Pcs. The shift of A and small satellites (s) might come from interface states formed upon orbital hybridization.

Figure 2 shows the observed θ (a) and ϕ (b) dependences of the band A (HOMO) and band B (HOMO-1) intensities, respectively. The θ pattern from B is rather similar to that of MnPc/HOPG, indicating the HOMO-1 is assigned to 2p-derived orbital (a_{1u}) as seen in other Pc/HOPG systems. We found that the deformation of the MO upon adsorption is surely occurring but not significant. The θ pattern for A (HOMO), however, is completely different from that of MnPc/HOPG, indicating that

the 3d-derived MO has changed. The electronic structure, especially 3d-derived MOs, of MnPc may be rearranged due to different spin configuration and/or change in the ligand field upon absorption. Now we are trying to obtain the angular dependences by using the multiple-scattering theory combined with MO calculation [3] under various spin configurations and MOs.
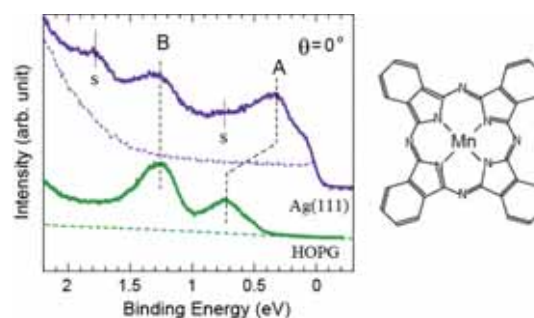

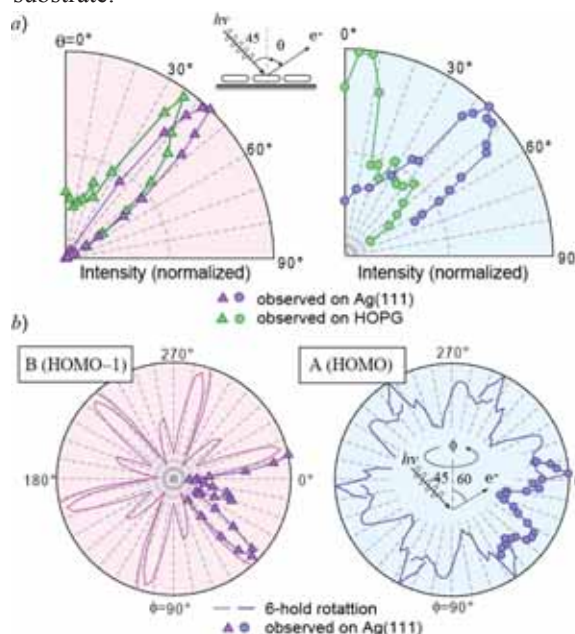Fig. 1. HeI UPS of 1-ML-MnPc on Ag(111) and HOPG. Both dashed curves are UPS from a clean substrate.

Fig. 2. (a) Observed θ patterns of band A (right) and B (left) obtained at $\alpha=45^{\circ}$, $\phi=0^{\circ}$. (b) Observed ϕ patterns of band A and B for MnPc/Ag(111) obtained at $\alpha=45^{\circ}$, $\theta=60^{\circ}$.

[1] N. Ueno *et al*, J. Chem. Phys. **107** (1997) 2079.
[2] S. Kera *et al*, UVSOR Activity Report 2006 (2007) 113.
[3] S. Nagamatsu *et al*, e-J. Surf. Sci. Nanotech, **3** (2005) 461.

6. SURFACE SCIENCE, PHOTOCHEMISTRY AND OTHERS

Interaction between Entrapped Atoms and C$_{78}$ Fullerene Cage

S. Hino [1], M. Kato[2], D. Yoshimura[3, 4], H. Moribe[5], H. Umemoto[5], Y. Ito[5], T. Sugai[5],
H. Shinohara[5], M. Otani[6], Y. Yoshimoto[6], S. Okada[7]

[1]*Graduate School of Materials Sci. & Biotech., Ehime Univ., Matsuyama 790-8577 Japan*
[2]*Graduate School of Sci. & Technology, Chiba Univ., Chiba 263-8522, Japan*
[3]*UVSOR, Institute for Molecular Science, Okazaki 444-8585, Japan*
[4]*Research Center of Material Science, Nagoya Univ., Nagoya 464-8602, Japan*
[5]*Graduate School of Science, Nagoya Univ., 464-8602, Japan*
[6]*Institute for Solid State Physics, Univ. of Tokyo, Kashiwa 277-8581, Japan*
[7]*Center for Computational Sciences, Univ. of Tsukuba, 305-8571 Tsukuba Japan*

Ultraviolet photoelectron spectra (UPS) of metallofullerene, La$_2$@C$_{78}$ that has D3h cage symmetry were measured using a synchrotron radiation light source [1]. The UPS are shown in Fig. 1. Its spectral onset energy was 0.70 eV below the Fermi level, indicating the semiconductive nature of this metallofullerene. The UPS consisted of numerous crests and troughs. Further, a change in intensity upon tuning the excitation energy was observed; however, the intensity of the change was not as large as those observed for other fullerenes. Previously measured UPS of Ti$_2$C$_2$@C$_{78}$ are also shown in Fig. 1 [2]. When the UPS of Ti$_2$C$_2$@C$_{78}$ were reported, it was thought that it was the mixture of two Ti$_2$@C$_{80}$ isomers, and it has been questioned that it is not the mixture but actually Ti$_2$C$_2$@C$_{78}$. Further it has been proposed that the cage symmetry of Ti$_2$C$_2$@C$_{78}$ is D_{3h}.

There are two so-called Isolated Pentagon Rule satisfying D3h cage structure in C$_{78}$ fullerene family. The UPS of La$_2$@C$_{78}$ differ considerably from those of Ti$_2$C$_2$@C$_{78}$, so that, at first, it was thought that these two metallofullerenes have different D_{3h} cage.

In order to examine this assumption, DFT calculation has been carried out in both cages with La$_2$ or Ti$_2$C$_2$ entrapped cages. Calculated DOS is shown in Fig. 1. Comparison revealed that both metallofullerenes have the same cage symmetry classified as D_{3h} (78:5) according to Fowler and Manolopoulos [3]. In most UPS of fullerenes, the UPS of the fullerenes having the same cage are analogous. Present results are rather extraordinary. Thus distribution of wave functions (DWF) in metallofullerenes is examined. Figure 2 shows the wave function distribution of HOMO and HOMO-1 orbitals of these two metallofullerenes.

DWF of the HOMO of both fullerenes is almost the same, but that of the HOMO-1 differs considerably: while HOMO-1 of La$_2$@C$_{78}$ distributes on the fullerene cage, that of Ti$_2$C$_2$@C$_{78}$ penetrates into the cage and tries to make hybridized bond with Ti atoms. Titanium has a tendency to form carbide. Possibly there might strong interaction between Ti atoms and cage constructing carbon atoms, and this is the reason why the same cage symmetry having La$_2$@C$_{78}$ and Ti$_2$C$_2$@C$_{78}$ give completely different UPS.
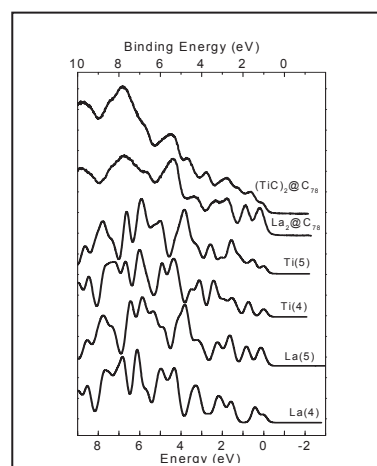

Fig. 1. UPS of La$_2$@C$_{78}$ and Ti$_2$C$_2$@C$_{78}$. Calculated DOS assuming La$_2$ or Ti$_2$C$_2$ species entrapped D_{3h} C$_{78}$ is also shown.
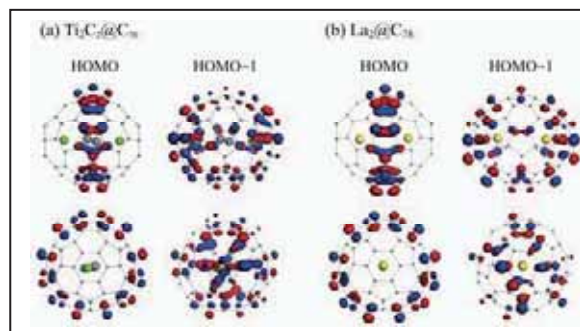

Fig. 2. Distribution of HOMO and HOMO-1 wave functions. Green circles indicate Ti, Yellow circles La, and grey circles C. Large grey circle indicate entrapped carbon atom.

[1] S. Hino *et al.*, Phys. Rev. B **75** (2007) 125418.
[2] K. Iwasaki *et al.*, Chem. Phys. Lett. **397** (2004) 169.
[3] P. W. Fowler, D. E. Manolopoulos, "An Atlas of Fullerenes", Oxford University Press, Oxford, 1995.

6. SURFACE SCIENCE, PHOTOCHEMISTRY AND OTHERS

Energy Level Alignment at PTCDA / Metal Interfaces

E. Kawabe[1], H. Yamane[1], R. Sumii[2,3], K. Koizumi[1], K. Kanai[2], Y. Ouchi[1], K. Seki[1]

[1]*Graduate School of Science, Nagoya University, Furo-cho, Chikusa-ku,*
Nagoya 464-8602 Japan
[2]*Research Center for Materials Science, Nagoya University,*
[3] *Present address: Photon Factory, Institute of Materials Structure Science, High Energy*
Acceleration Research Organization, Oho 1-1, Tsukuba, 305-0801 Japan

Recently extensive research has been carried out for applying organic materials to electronic devices. It is important to understand how the energy levels align at organic / metal (O / M) interfaces for improving their performance. However, the detailed mechanism of the energy level alignment at O / M interface is still unclear. Vázquez *et al*. proposed the induced density of interface states (IDIS) model [1] to theoretically explain the vacuum level (VL) shift at O / M interface [2, 3]. They made several assumptions to simplify the calculation, i.e. (1) the energy levels of the highest occupied molecular orbital (HOMO) and the lowest unoccupied molecular orbital (LUMO) are broadened to form continuous levels, which is called the IDIS by the interaction with the metal state, (2) only the s-state is taken into account as the metal state. Although this model well explains the observed Δ at organic / Au interfaces, it has been still unclear whether this model can be generally applied to various metal substrates. Thus we investigated the energy level alignment at the interfaces between perylene-3, 4, 9, 10-tetracarboxylic dianhydride (PTCDA, Fig. 1) and metals (Au, Ag and Cu) by ultraviolet photoelectron spectroscopy (UPS).

The plot of the observed Δ as a function of the metal work function (Φ_M) is shown in Fig. 1. In the IDIS model, it is expected that Δ and Φ_M show a linear relation. However, we cannot see such relation. The UPS spectra of monomolecular layer (1 ML) PTCDA film on Au(111), Ag(111) and Cu(111) are shown in Fig. 2. The interface states are observed for Ag and Cu interfaces, and they are not the broadened states but the split stat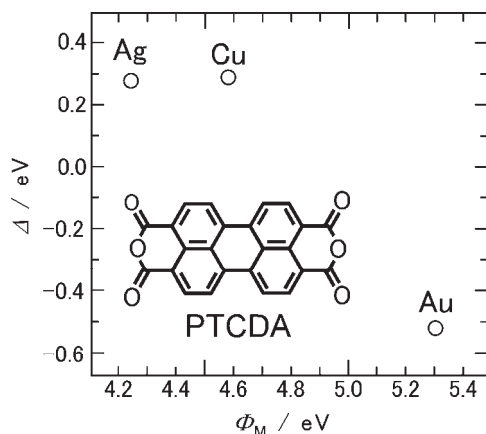es. These results indicate that the IDIS model cannot be applied to these interfaces, and that the interaction with the metal d-band states cannot be neglected.

Then we estimate the interface interaction by taking into account the metal d-band states. We expect that [5] the magnitude of the attractive interaction depends on the inverse of the energy separation between the LUMO of PTCDA and the centroid of the metal d-band ($\varepsilon_{d\text{-LUMO}}$), and that the magnitude of the repulsive interaction depends on the coupling matrix element (V) between the adsorbate state and the metal d-band state. The value of $\varepsilon_{d\text{-LUMO}}$ for the PTCDA / Cu interface is the smallest. The value of V for the PTCDA / Au interface is the largest, since V increases with the principal quantum number. From these results, it is found that the interaction for the Au interface is very weak (physisorption), and those for the Ag and Cu interfaces are strong (chemisorption). These results indicate that the observed VL shift for the Au interface is due to the rearrangement of the surface electron cloud at the Au surface by the push-back effect, and those for the Ag and Cu interfaces are due to the formation of the interface states resulting in the charge redistribution ate the interfaces.
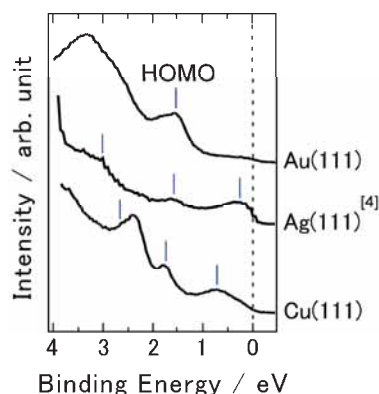

Fig. 2. UPS spectra of 1 ML PTCDA / metal interfaces.

[1] H. Vazquez *et al*., Europhys. Lett. **65** (2004) 802.
[2] S. Narioka *et al*., Appl. Phys. Lett. **67** (1995) 1899.
[3] H. Ishii *et al*., Adv. Mater. **11** (1999) 605.
[4] Y. Zou *et al*., Surf. Sci. **600** (2006) 1240.
[5] A. Ruban *et al*., J. Mol. Catal. A: Chem. **115** (1997) 421.

Fig. 1. Plot of Δ as a function of Φ_M. Inset: Molecular structure of PTCDA.

6. SURFACE SCIENCE, PHOTOCHEMISTRY AND OTHERS

Valence Electronic Structure of Metal Phthalocyanine Monolayers on Graphite

S. Kera[1], T. Aoki[1], S. Hosoumi[1], N. Mitsuo[1], K. Nebashi[1], T. Kataoka[1], R. Sumii[2], S. Nagamatsu[1], N. Ueno[1]

[1]Graduate School of Advanced Integration Science, Chiba University, Chiba 263-8522 Japan
[2]Graduate School of Science, Nagoya University, Nagoya 464-8602 Japan

Angle-resolved ultraviolet photoelectron spectroscopy (ARUPS) has been known as a powerful technique to obtain crucial information on electronic band structure for various kinds of materials. Moreover, for organic thin films, information on the molecular orbital (MO) character, bonding nature, can be also discussed in accordance with a quantitative analysis of the ARUPS intensity using photoelectron scattering theory when the geometrical structure of the thin films are considered.

Phthalocyanines(Pcs) are a versatile class of π-conjugated organic semiconductors applicable as device materials. Among these the transition metal Pcs are interesting materials in controlling the device performance via 3d-electron derived MOs. However, information on the electronic structure of these organometallic complexes is still limited. Here, we show the electronic structure of the monolayer of various transition metal (Mn-, Fe-, Co-, Ni-) Pcs on graphite systematically.

The observed electron emission angle (θ) dependences of 2p- and 3d-orbital derived MO bands in ARUPS spectra for well-ordered Pc monolayers were compared.

Experimental

ARUPS spectra were measured at photon incidence angle α=45°, hν=28 or 30 eV, and a sample temperature T=295 K. θ dependence of ARUPS spectra was analyzed using the multiple-scattering theory combined with molecular orbital (MST/MO) calculation [1]. The purified Pc molecules were carefully evaporated onto the graphite (HOPG: grade ZYA). We have found that the molecules are oriented nearly flat to the substrate surface [2].

Results and Discussion

Figure 1 shows θ dependence of ARUPS of annealed-Pc monolayers (MnPc, FePc, CoPc and NiPc) on HOPG. The intensity is normalized to the incidence photon flux. DFT-MO calculation suggests that (i) features A are ascribed to 3d-derived band of Pcs and (ii) features B are assigned to 2p-derived band (a single π MO). Note that the MO calculation to discuss the electronic structure still may have difficulties for organometallic complexes.

Figure 2 shows the comparison between observed and calculated θ dependences of the band A and B intensities for MnPc, CoPc and NiPc (FePc is still under analysis). The θ patterns are completely different between 3d- (A) and 2p-derived (B) bands. In the fitting for π bands (B), the observed θ patterns

are well reproduced by the MST/MO calculation of a free molecule for MO (π: a_{1u}), while for 3d-derived bands (A), the observed θ patterns are not fitted by the calculation from MO (3d: a_{1g}). Note that the θ pattern of MO (3d: a_{1g}) depends on the strength of the metal-ligand bonding, that is, on the hybridization between 3d and 2p orbitals.

The results indicate that the 3d-derived band is located at various energy positions due to change in the 3d-electron occupation, while 2p-derived (π) band appears at the similar energy. Further analysis on the intensity of feature A is necessary.

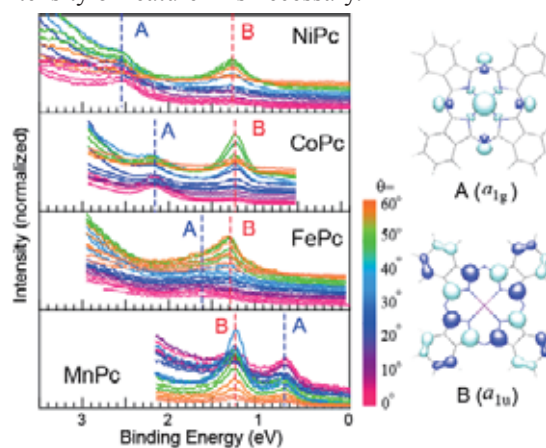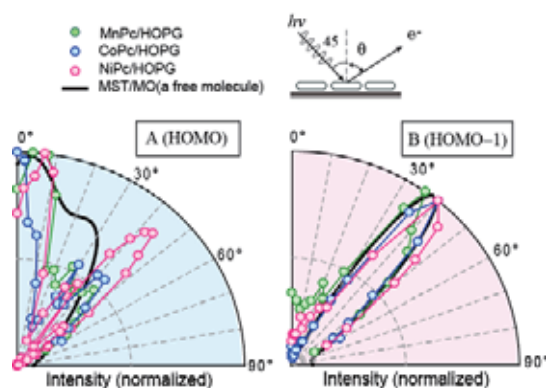Fig. 1. θ dependences of ARUPS of 1-ML-Pcs (MnPc, FePc, CoPc and NiPc) on HOPG. MOs calculated for CoPc are also shown.

Fig. 2. Comparison between the observed and calculated θ patterns of the band A (left) and B (right).

[1] S. Nagamatsu *et al*, e-J. Surf. Sci. Nano **3** (2005) 461.
[2] T. Kataoka *et al*, Chem. Phys. Lett. **451** (2008) 43.

Angle-Resolved UPS of Thin Films of *o*-Quinonate Complex on Graphite

N. Mitsuo[1], T. Aoki[1], Y. Suzuki[1], S. Nagamatsu[1], R. Sumii[2], S. Noro[3], T. Hosokai[1],
K. K. Okudaira[1], N. Ueno[1], S. Kera[1]

[1]*Graduate School of Advanced Integration Science, Chiba University, Chiba 263-8522 Japan*
[2]*Graduate School of Science, Nagoya University, Nagoya 464-8602 Japan*
[3]*Research Institute for Electronic Science, Hokkaido University, Sapporo 060-0812, Japan*

Bis-(*o*-diiminobenzosemiquinonate) nickel(II) complex {Ni(DIBSQ)} is known to have a narrow band-gap of 0.8 eV. Recently, high-performance ambipolar operation in organic field effect transistor of Ni(DIBSQ) was reported [1].

We have investigated the electronic structure and molecular orientation of Ni(DIBSQ) in a thin film by using angle-resolved ultraviolet photoelectron spectroscopy (ARUPS). ARUPS has been known as a powerful technique to obtain crucial information on electronic band structure for various kinds of materials. Moreover, for organic thin films, information on the geometrical structure of the thin films can be also discussed in accordance with a quantitative analysis of the ARUPS intensity using photoelectron scattering theory.

In this report, we show the observed electron-emission-angle (θ) dependence of HOMO bands in ARUPS spectra for the standing Ni(DIBSQ) layer deposited on a graphite substrate.

Experimental

ARUPS spectra were measured at photon incidence angle $\alpha=45^{\circ}$, hν=40 eV, and T=295 K. The purified molecules were carefully evaporated onto the graphite (HOPG) substrate. θ dependence was analyzed using the multiple-scattering theory combined with molecular orbital (MST/MO) calculation [2].

Results and Discussion

Figure 1(a) shows the θ dependence of ARUPS of Ni(DIBSQ) (3.5nm) on the HOPG. The intensity is normalized to the incidence photon flux. A top feature appeared around 1.4 eV is ascribed to HOMO band of Ni(DIBSQ). One can see an energy shift of the HOMO about 280 meV depending on the θ (see the guide lines). We found that the molecules are oriented nearly standing to the substrate surface from NEXAFS results (as shown in the right panel in Fig.1). Accordingly we expect that the DOS structure in the HOMO feature of UPS, which comes from the HOMO band dispersion, could be observed even for polycrystalline Ni(DIBSQ) films as in pentacene [3]. ARUPS study for the standing film on the single crystal would be fascinating.

Figure 1(b) shows the comparison between observed and calculated θ dependences of the HOMO intensity. The observed intensity gives the maximum at around 0°. There are large differences between observed and calculated MST/MO patterns. Here we

performed the MST/MO calculation for a unit model of 5 molecules to describe the intermolecular scattering effects. We also found that the observed θ pattern depends on the photoelectron kinetic energy and the sample quality (molecular packing and/or crystallinity). These indicate that the impacts of the interference of scattered photoelectron waves are crucial. We are trying to compute the angular dependence by taking into account the intermolecular layer effects.
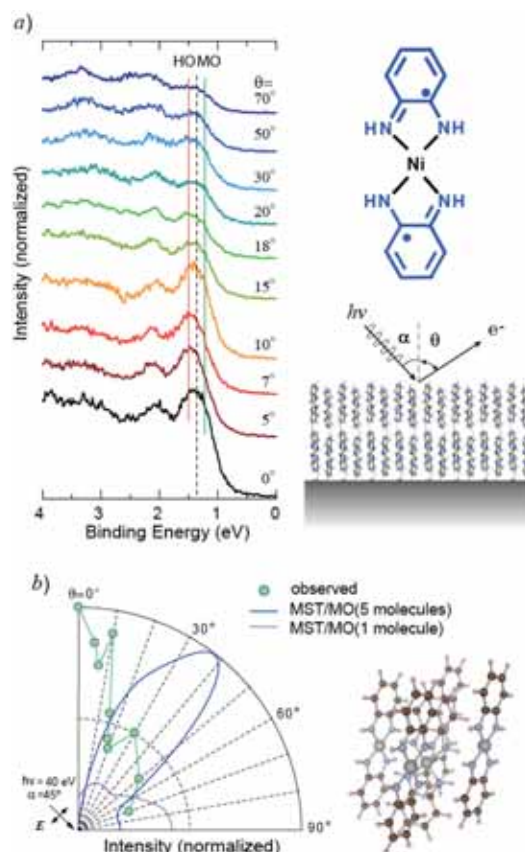

Fig. 1. a) θ dependence of ARUPS of Ni(DIBSQ) on HOPG, b) Observed and calculated θ patterns of the HOMO. Chemical structure, schematic view of the film structure, and a unit model for the calculation are also shown.

[1] S. Noro *et al*, J. Am. Chem. Soc. **127** (2005) 1001.
[2] S. Nagamatsu *et al*, e-J. Surf. Sci. Nanotech, **3** (2005) 461.
[3] H. Fukagawa *et al*, Phys. Rev. B **73** (2006) 245310.

6. SURFACE SCIENCE, PHOTOCHEMISTRY AND OTHERS

Electronic Structure of LiNi$_{1-x}$M$_x$O$_2$ Mixed Oxides (III)

T. Miyazaki[1], R. Sumii[2,3], T. Kamei[1], H. Tanaka[1], S. Hino[1]

[1]*Graduate School of Science and Engineering, Ehime University, Matsuyama 790-8577, Japan*

[2]*Research Center for Materials Science, Nagoya University, Nagoya 464-8602, Japan*

[3]*UVSOR Facility, Institute for Molecular Science, Okazaki 444-8585, Japan*

Hexagonal lithium nickel oxide (LiNiO$_2$) is active for the oxidation coupling of the methane (OCM) with a selective function of oxidation catalyst. We have studied the crystal structure and the surface oxygen species for understanding the selective oxidation mechanism and synthesized hexagonal Li-Ni mixed metal oxides (LiNi$_{1-x}$M$_x$O$_2$; M=transition metal). The OCM activity of LiNi$_{1-x}$Ti$_x$O$_2$ (0.05≤x≤0.2), which was replaced Ti with a part of Ni of LiNiO$_2$, increased by the metal substitution. In this study, the UPS spectra of LiNi$_{0.95}$Ti$_{0.05}$O$_2$ and LiNi$_{0.995}$Ti$_{0.005}$O$_2$ were measured with the dependence of the incident photon energy. In addition, the change of the UPS spectra of LiNiO$_2$ thin film was reported by the difference of pre-treating of the sample.

LiNi$_{0.95}$Ti$_{0.05}$O$_2$ and LiNi$_{0.995}$Ti$_{0.005}$O$_2$ were synthesized by solid state reaction. LiNiO$_2$ thin film was synthesized by Li ion diffusion on Ni plate. The UPS spectra were measured at BL8B2 of UVSOR in Institute for Molecular Science. The argon ion sputtering and IR heating of samples were done in order to imitate rough surface and remove the contamination.

Figure 1 was shown the UPS spectra of LiNiO$_2$ thin film at hν = 40eV. The valence band spectra consist of five structures at E$_b$≤15eV below the Fermi level. The top valence region was almost derived from the Ni3d and O2p states. After the heat treatment the intensity of Ni3d states decreased, but the features of two O2p peaks were cleared. It was analogized that two kinds of oxygen species existed and functioned for the selective oxidation. Figure 2 was shown the UPS spectra of LiNi$_{0.95}$Ti$_{0.05}$O$_2$ and LiNi$_{0.995}$Ti$_{0.005}$O$_2$ of the incident photon energy at 20-60eV. The valence band spectra of LiNi$_{0.95}$Ti$_{0.05}$O$_2$ and LiNi$_{0.995}$Ti$_{0.005}$O$_2$ also consist of five structures in this region. The UPS spectral features of LiNi$_{0.995}$Ti$_{0.005}$O$_2$ were analogous to those of hexagonal LiNiO$_2$. In the case of LiNiO$_2$ and LiNi$_{0.995}$Ti$_{0.005}$O$_2$, the UPS spectra caused the intensity change which depended on the incident photon energy, but only small spectral change of LiNi$_{0.95}$Ti$_{0.05}$O$_2$ was observed at 20-60eV. It was speculated that the valence band feeling might be changed by replacing Ti^{4+} in Ni^{3+}.

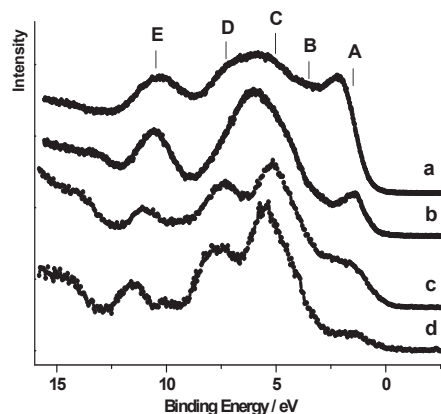Fig. 1. The UPS spectra of thin film LiNiO$_2$ samples, a) Ar ion sputtering, b) Heating with O$_2$ at 450℃, c) 450℃ under 10^{-6} Pa, d) 600℃ under 10^{-6} Pa.
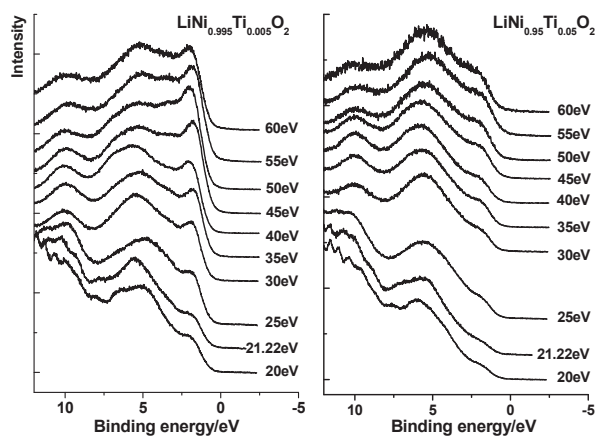
Fig. 2. The UPS spectra of LiNi$_{0.995}$Ti$_{0.005}$O$_2$ and LiNi$_{0.95}$Ti$_{0.05}$O$_2$ with the dependence of the incident photon energy at 20-60eV.

Electronic Structures of Rubrene and Its Photooxidation Product

Y. Nakayama[1], S. Machida[2], T. Minari[3], K. Tsukagoshi[3], H. Ishii[1,4]

[1]*Center for Frontier Science, Chiba University, Chiba 263-8522 Japan*
[2]*Faculty of Engineering, Chiba University, Chiba 263-8522 Japan*
[3]*Nanoscience Development and Support Team, RIKEN, Saitama 351-0198 Japan*
[4]*Graduate School of Advanced Integration Science, Chiba University, Chiba 263-8522 Japan*

Introduction

Rubrene (5,6,11,12-tetraphenyltetracene) is one of the most promising candidates for a *p*-type organic field effect transistor owing to a high hole mobility in its single-crystalline (SC) phase [1]. Since rubrene easily reacts with oxygen to form its *endo*-peroxide (RubO$_2$) under visible light illumination (Fig.2 inset), it is believed that the surface of rubrene SC is covered with "native" oxide layers and the oxidized product also contributes to the conduction mechanism as a dopant [1,2]. Toward understanding on the transport nature and further improvement of the device performance, information about the electronic structure of not only the pristine rubrene but also its photooxidation product is indispensable.

In the present study, we conducted photoelectron spectroscopy (PES) and photoelectron yield spectroscopy (PYS) measurements for a thin film of rubrene before and after the photooxidation reaction.

Experiment

An amorphous film of rubrene was made on indium-tin-oxide (ITO) by *in-situ* vacuum sublimation. RubO$_2$ was produced by exposing the rubrene film to ambient air under illumination of room light for 3 days. PES measurements were conducted at BL8B2. All the PES spectra presented below were taken at normal emission angle ($h\nu = 40$ eV). The Fermi-level position was determined from a gold foil. The work function of each sample was estimated from the secondary electron cut-off taken at the sample bias of –5 V. PYS measurements were performed by a home-built system [3].

Results and discussion

Figure 1 shows PES spectra of the pristine rubrene film and the photooxidized film. The peak corresponding to the highest occupied state of rubrene, which is assigned to the tetracene backborn, disappears after photooxidation. It is in good agreement with the previous report for a RubO$_2$ film oxidized in pure oxygen [4]. As shown in Fig. 2, the ionization potential (I_s) estimated from the PES matches that from PYS results in cases of the pristine film and RubO$_2$. No clear sign of the oxidation induced midgap state [2] was identified.

We also conducted PES measurement of a rubrene SC. For SC, however, features at the binding energy (E_b) below 6 eV are absence, and apparent I_s's are completely different between PES and PYS results.

Two factors should be taken into account on considering the PES spectra of rubrene SC: the one is surface oxidation, and the other is sample charging. Note that probing depth of PYS is much greater than PES because PYS detects photoelectrons of extremely slow (typically less than 1 eV). Removal of the oxidation product by vacuum heating [4] and/or vacuum cleavage of the crystal will possibly enable us to observe the PES spectra of "pristine crystal" covered with the oxide. Trials to avoid the sample charging problem such as visible light irradiation are now underway.
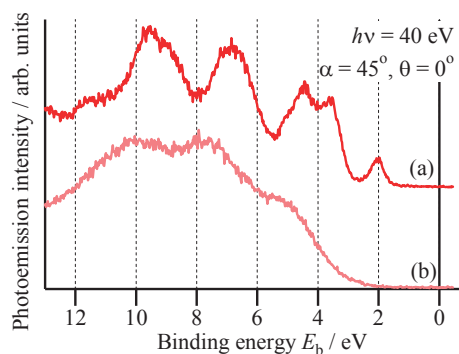

Fig. 1. PES spectra of (a) the pristine rubrene film and (b) the RubO$_2$ film.
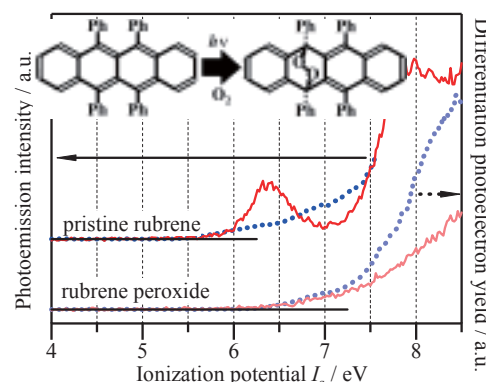
Fig. 2. Magnified PES spectra near the HOMO region (lines, left axis) and differentiation intensity of PYS spectra (dots, right axis). [Inset] Molecular structures before and after the photooxidation.

[1] V. Podzorov, *et al.*, Appl. Phys. Lett. **85** (2004) 6039.
[2] O. Mitrofanov, et al., Phys. Rev. Lett. **97** (2006) 166601.
[3] H. Ishii, *et al.*, Hyomen-kagaku **28** (2007) 264.
[4] Y. Harada, *et al.*, Chem. Phys. Lett. **62** (1979) 283.

6. SURFACE SCIENCE, PHOTOCHEMISTRY AND OTHERS

ARUPS of Diabenzo-Crown Ether Thin Film on HOPG

K. K.Okudaira[1], T. Hosokai[2], Y. Suzuki[1], S. Kera[1], N. Ueno[1]

[1]*Association of Graduate Schools of Science and Technology, Chiba Univererity,1-33 Yayoi-cho Inage-ku, Chiba 263-8522, Japan*

[2]*Graduate School of Science and Technology, Chiba Univererity,1-33 Yayoi-cho Inage-ku, Chiba 263-8522, Japan*

Introduction

Crown ethers, which consist of flexible oligo-ethers, have remarkable properties of recognizing and binding specific metal atoms, and thus have potential for use in molecular mechanics. [1] In particular, dibenzo-18-crown-6(2,3,11,12–dibenzo-1,4,7,10,13,16- hexaoxacyclo- octadeca- 2,11-diene) (DB18C6), forms a self-organized two-dimensional structure of a Au(111) substrate in $HClO_4$ solution. [2] The DB18C6 has a non-planar and flexible molecular structure, shown in Fig.1.

In this study, we report the results of angle resolved ultraviolet photoelectron spectra (ARUPS) of DB18C6 thin films on HOPG to determine the molecular orientation of DB18C6 thin films quantitatively.
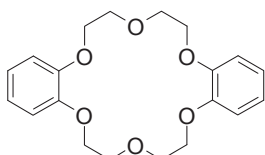
Experimental

Fig. 1. Molecular structure of DB18C6.

ARUPS measurements were performed at the beam line BL8B2 of the UVSOR storage ring at the Institute for Molecular Science. The take-off angle (θ) dependencies of photoelectron spectra were measured at grazing incidence (incident angle of photon (α) = 70° with the photon energy of 20 eV.
The thin films were prepared in the preparation chamber by vacuum evaporation onto HOPG surfaces which were cleaved under an ultrahigh vacuum. The deposition rate was smaller than 0.1nm /min..

Results and Discussion

The θ dependencies of ARUPS spectra of about 2nm thick film at the binding energy region of 0-5 eV are shown in Fig. 2, where three bands A, B, and C appear. From the comparison of the results of molecular orbital calculation, band A and B are ascribed to the π-orbitals of benzene rings, and band C are n(O) localized at an ether ring.[3] The intensity of the band A, B and C depends on θ, while the energy positions of these bands do not.

The band A, B, and C intensities show characteristic θ dependencies (Fig.3), which reflect the molecular orientation of DB18C6 thin films on HOPG. To determine the molecular orientation quantitatively, it needs to compare the observed θ dependencies with the calculated ones.
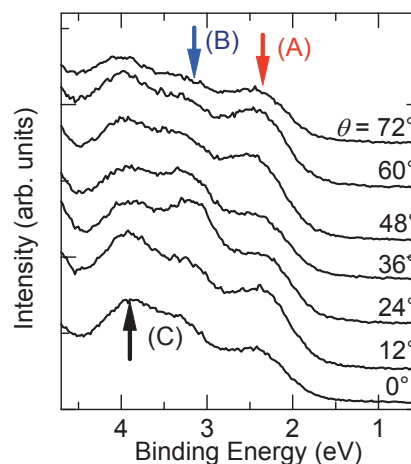
Fig. 2. Take-off angle dependence of ofDB18C6 (three arrows indicate the peak position of A, B, and C).

Fig. 3. Take-off angle (q) dependencies of photoelectron intensities of peak A (●), B(●), and C(●).

[1] C. J. Pedersen, J. Am, Chem. Soc. **89** (1976)2495.
[2] A. Ohira, M. Sakata, C. Hirayama, M. Kuntake, Org. Biomol. Chem. **1** (2003) 251.
[3] T. Hosoaki, H. Horie, T. Aoki, S. Nagamatsu, S. Kera, K. K. Okudaira, N. Ueno, J. Phys. Chem. C, *to be published*.

Electronic Structure of Molecular Crystal with CN-I Interaction
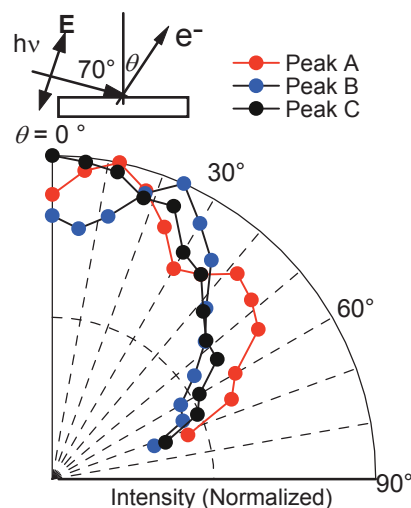
R. Sumii[1,2], K. Kanai[2], K. Seki[3]

[1]*Institute of Materials Structure Science, High Energy Accelerator Research Organization, Tsukuba, Ibaraki 305-0801, Japan*
[2]*Research Center for Materials Science, Nagoya University, Nagoya 464-8602, Japan*
[3]*Department of Chemistry, Nagoya University, Nagoya 464-8602, Japan*

Introduction

Some halogen containing molecules, such as *p*-iodo- benzonitrile (*p*-IBN) (Fig. 1(a)), are known to show strong intermolecular interaction. *p*-IBN molecule has a simple structure with I and CN at the opposite sides of a benzene ring. In the crystal, the *p*-IBN molecules form straight chains with CN-I distance nearly 7% shorter than the sum of the van der Waals radii [1]. Thus we can expect that interesting phenomena such as intermolecular charge transfer and anisotropic electrical conductivity may occur in crystals with such CN-I interaction. However, there have been little studies of the electronic structure and electrical properties. The main reason may be sublimation by high vapor pressure in vacuum condition required in such studies and the dissociation of the I-C bond at the contact with clean metal surface.

To solve these problems, in this work we chose a new compound 4-cyano-4'-iodobiphenyl (CIB) and studied the electronic structure of the vacuum deposited thin film by ultraviolet photoemission spectroscopy (UPS). In CIB molecule, the benzene ring of *p*-IBN is substituted with biphenyl (Fig. 1(b)). Like *p*-IBN, the distance between the CN-I is about 5 % shorter than the sum of van der Waals radii and the crystal structure contains straight chains [2]. Moreover, the molecular weight is heavier than *p*-IBN, hindering the sublimation in vacuum. For suppressing possible dissociation by the contact with metal substrate, we used GeS (001) which is an inactive substrate.
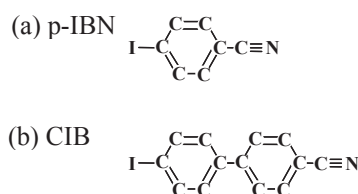
(a) p-IBN

(b) CIB

Fig. 1. Molecular structures of IBN and CIB.

Experimental and Theoretical

The CIB film was deposited on a clean GeS (001) surface obtained by cleaving in the vacuum chamber. UPS measurements were performed at BL-8B2 of the UVSOR facility. Molecular orbital (MO) calculations were performed by density functional theory with Gaussian98 package using a B3LYP / 3-21G** basis set.

Results and Discussion

The observed spectra of CIB on GeS (001) and the simulated spectra based on the MO calculations are shown in Fig. 2. In the experimental results, the HOMO at around 3 eV shifts to low binding energy as the film thickness increases,. This shift is well reproduced by MO calculations for molecular chains with increasing length from monomer to tetramer, simulating the formation of crystal structure. For the dimmer, calculations were also performed for various CN-I bond lengths.
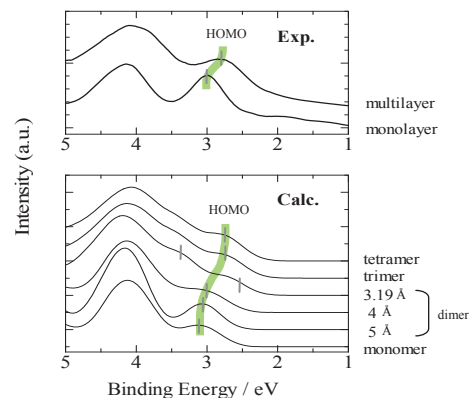

Fig. 2. Experimentally observed UPS spectra and the simulated spectra by the MO calculations for CIB.

Such good correspondence between the observed spectra and the results of MO calculations indicate that the HOMO shift is due to the intermolecular interaction through the CN-I contact. As the detailed mechanism, the HOMO with large component at the iodine is pushed up by the negative charge at the CN part in the neighboring molecule (Fig. 3).
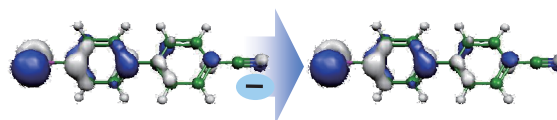

Fig. 3. Unstabilization of the HOMO by the negative charge at the CN group of the neighboring molecule .

[1] E. O. Schlemper, Acta. Cryst. **18** (1965) 419.
[2] D.Britton, Acta. Cryst. **C47** (1991) 2127.

6. SURFACE SCIENCE, PHOTOCHEMISTRY AND OTHERS

Photoelectron Spectroscopy Study of Photochromic Diarylethene Film

S. Tanaka[1], M. Toba[2], T. Nakashima[2], T. Kawai[2], K. Yoshino[3]

[1]*Center of Integrated Research in Science, Shimane University, Matsue 690-8504, Japan*
[2]*Graduate School of Materials Science, Nara Institute of Science and Technology, NAIST, Ikoma, Nara 630-0192, Japan*
[3]*Shimane Institute for Industrial Technology, Matsue, Shimane 690-0816 Japan*

Photochromic molecules have attracted much attention as a promising material for photonic devices. Photochromism is defined as the reversible transformation between two isomers having different absorption spectra by photoirradiation.[1] In addition, the geometry and electronic structures in two isomers of the photochromic molecules are also different. The differences in the geometry and the electronic structure relate to the difference in the molecular properties, such as refractive index, fluorescence efficiency, conductivity and magnetism reference. These photoresponsive variations of the molecular properties can be useful for the application to various optoelectronic devices. Among the various photochromic materials, diarylethenes with heterocyclic aryl groups are of particular interest for applications to optoelectronic devices because of their high fatigue resistance and good thermal stability [1]. 1,2-Bis(5-(2,4-diphenylphenyl)-2,4-dimethyl-3-thienyl) perfluorocyclopentene (DAE) is a dithienylethene derivative having bulky substituents [2]. DAE shows blue coloration upon UV light irradiation, and the blue color disappears upon visible (λ > 450 nm) light irradiation. It is known that DAE undergoes ring cyclization and cycloreversion reactions upon alternate irradiation with UV and visible light (Fig. 1). Hereafter, open-DAE and close-DAE refer to the open- and the closed-ring form isomers, respectively.
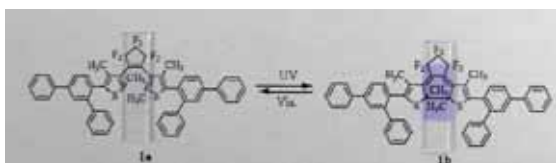

Fig. 1. Molecular structures of open-ring isomer of DAE (left) and closed-ring isomer of DAE (right). The arrows indicate the reversible electrocyclic reaction upon alternate irradiation with UV and visible light.

In this study, the electronic structure of the DAE thin film is revealed using photoelectron spectroscopy. The photoelectron spectra of open- and close-DAE showed clear differences in the density of states around the highest occupied molecular orbital (HOMO). The energy levels of each of the DAE molecules were calculated by the density functional theory (DFT) and it showed good correlation with the photoelectron spectra [3].

The vacuum-deposited DAE film was investigated by photoelectron spectroscopy. The structure of the as-deposited DAE film was considered amorphous. Figure 2 shows the photoelectron spectra of DAE after UV light irradiation (red) and under laser light irradiation (black). The UV lamp was used to induce a coloration of the DAE film. The majority state of the DAE molecule after UV light irradiation was able to assume close-DAE. In the red-line spectrum, a peak that appeared at around 1.5 eV was considered as the photoelectron from HOMO of close-DAE. The black-line in Fig. 2 is a photoelectron spectrum of the DAE under laser light irradiation, where the majority state was considered as open-DAE. It is obvious that the signal intensity around 1.5 eV was decreased compared with the red-line. The spectrum shape around 2 - 4 eV also showed a clear difference. The signal intensity at around 3 eV in the black-line spectrum was larger than that in the red-line spectrum. The appearance and the disappearance of the HOMO peak at 1.5 eV showed good relationship with UV and laser light irradiation, respectively. These variations in the spectra are attributed directly to the photoresponsive change in the electronic structure of DAE.
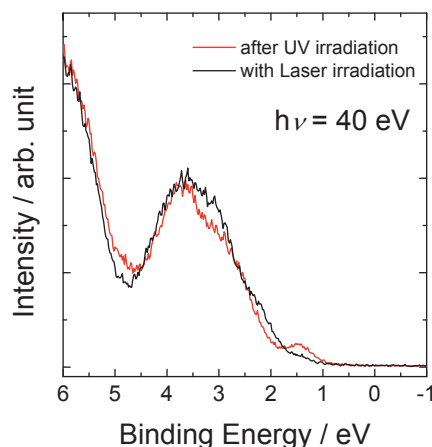

Fig. 2. Photoelectron spectra of DAE.

[1] M. Irie, Chem. Rev. **100** (2000) 1685.
[2] M.-S. Kim, T. Sakata, T. Kawai, M. Irie, Jpn. J. Appl Phys. **42** (2003) 3676.
[3] S. Tanaka, M. Toba, T. Nakashima, T. Kawai, K. Yoshino, Jpn. J. Appl. Phys. **47** (2008) 1215.

Intermolecular Energy Band Dispersion in Highly Ordered Pentacene Multilayer Films on Cu(110)

H. Yamane[1], E. Kawabe[1], R. Sumii[2], K. Kanai[2], Y. Ouchi[1], K. Seki[1]

[1]*Department of Chemistry, Nagoya University, Nagoya 464-8602, Japan*
[2]*Research Center for Materials Science, Nagoya University, Nagoya 464-8602, Japan*

Introduction

The energy band dispersion, $E(\boldsymbol{k})$, is a fundamental basis for understanding charge transport mechanisms of solids. In the field of organic solids, there are two types of band dispersion; the *intra-* and *inter-*molecular band dispersions. In particular, the issue of intermolecular band dispersion is attracting growing attention due to the needs of the interpretation of the charge transport mechanism in (opto)electronic devices using organic semiconductors such as field effect transistors. It is reported that molecules of pentacene (Pn), a high hole mobility material, deposited on Cu(110) in the multilayer regime (more than 10 nm) form a highly ordered structure with an upright-standing orientation, which is virtually identical to the herringbone orientation for Pn films on quartz or polyester substrates [1]. In this work, in order to understand the hole transport mechanism in Pn films, we studied the electronic structure of the highly ordered upright-standing Pn multilayer film on Cu(110) by using angle-resolved UV photoemission spectroscopy (ARUPS).

Experiment

The highly ordered Pn multilayer film was prepared on the clean Cu(110) surfaces in accordance with the sample preparation described in Ref 1.

The photoelectron takeoff angle (θ) dependence of ARUPS spectra was measured at the photon energy of 20 eV, the photon incidence angle of 60° from the surface normal, and the temperature of 300 K.

Results and Discussion

Figures 1(a) and (b) shows the θ dependence of the ARUPS spectra for the 11-nm-thick Pn multilayer film with the upright-standing orientation along (a) the $\bar{\Gamma}-\bar{X}_{Pn}$ direction ($\phi = 0°$), and (b) the $\bar{\Gamma}-\bar{Y}_{Pn}$ direction ($\phi = 90°$). At $\theta = 0°$, the topmost peak consists of two prominent components with an energy separation of 0.5 eV (labelled H_1 and H_2 in Fig. 1, respectively). This lineshape shows continuous change with θ. At $\phi = 0°(90°)$, H_1 shifts to the high E_b side until θ reaches 18°(12°), and turns to the low E_b side until θ reaches 34°(26°). Such a dispersive behaviour can also be seen in H_2. As shown in Fig. 1 (c) and (d), the observed shifts can be explained as the reflection of the two-dimensional intermolecular band dispersion using the unit cell of the upright-standing Pn multilayer film on Cu(110) [2], which was obtained from the previous structural studies [1].
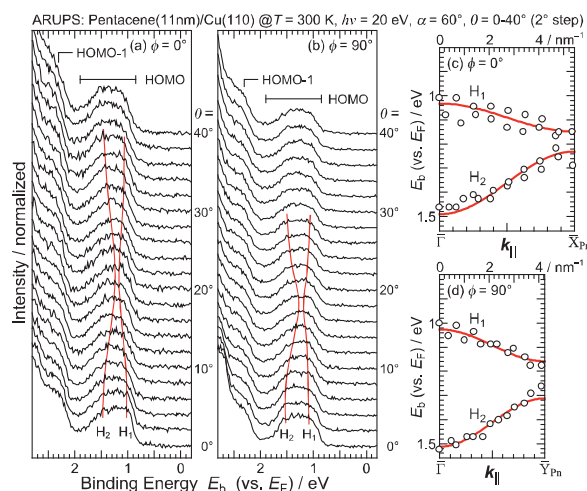

Fig. 1. (a,b) Photoelectron takeoff angle (θ) dependence of the ARUPS spectra for the highly ordered upright-standing Pn multilayer film on Cu(110) measured at $\phi =$ (a) 0° and (b) 90°. The abscissa is the binding energy (E_b) relative to the Fermi level (E_F) of the substrate, and ordinate is the intensity of the photoelectron, normalized by the incident photon flux. (c,d) $E(\boldsymbol{k}_\parallel)$ relation for the highly ordered upright-standing Pn multilayer film on Cu(110) at $\phi =$ (c) 0° and (d) 90°. The abscissa is the parallel component of the momentum ($\boldsymbol{k}_\parallel$), and ordinate is the E_b relative to the E_F of the substrate.

From the observed $E(\boldsymbol{k}_\parallel)$ relation, one can see that the phase of the dispersion for band H_1 is opposite to that for band H_2, and that the size of the dispersion of bands H_1 and H_2 are about 150 and 240 meV, respectively, for both azimuths within the present total energy resolution of 100 meV at 300 K. Since the uppermost band H_1 seems to form a free-electron-like parabolic dispersion, we estimated the effective mass m_h^* to be $3.02m_0$ ($\bar{\Gamma}-\bar{X}_{Pn}$) and $1.86m_0$ ($\bar{\Gamma}-\bar{Y}_{Pn}$) at 300 K. This result demonstrates the presence of the anisotropy of the hole mobility in Pn crystals also at higher temperatures as suggested by Wijs *et al.* [3].

[1] S. Söhnchen *et al.*, J. Chem. Phys., **121** (2004) 525.
[2] H. Yamane *et al.*, Phys. Stat. Sol. (b), **245** (2008) 793.
[3] G. A. de Wijs *et al.*, Synth. Met., **139** (2003) 109.

Organic/Metal Interface State: Broadening and Splitting Behaviors of Molecular Energy Levels

H. Yamane[1], E. Kawabe[1], R. Sumii[2], K. Kanai[2], Y. Ouchi[1], K. Seki[1]

[1]*Department of Chemistry, Nagoya University, Nagoya 464-8602, Japan*
[2]*Research Center for Materials Science, Nagoya University, Nagoya 464-8602, Japan*

Introduction

The electronic structure at organic(O)/metal(M) interfaces plays a crucial role in the performance of organic electronic devices. In particular, the energies of the highest-occupied and lowest-unoccupied molecular orbital (HOMO and LUMO) levels relative to the Fermi level (E_F) of metals are of fundamental importance in discussing the barrier heights for the charge injection and separation at O/M interfaces. This is still an issue of open question since the interfacial electronic structure is usually modified by various interface-specific phenomena. For deeper understanding of the O/M interface energetics, one of the keys is the elucidation and control of the interface state near E_F, which may dominate the energy level alignment at the interface.

In this work, we studied the electronic structure of various pentacene (Pn) monolayers grown on Au(111), Cu(111), Cu(100), and Cu(110) surfaces using angle-resolved UV photoemission spectroscopy (ARUPS). We observed the evidences of the formation of the interface state, which depends on the type of the metal and its surface structure.

Experiment

All Pn monolayers were prepared on the clean metal surfaces at the temperature of about 500 K, which realizes the formation of flat-lying Pn mono-layers. The ARUPS measurements were performed at the surface temperature of 300 K at the photon energy of 20 eV and the photon incidence angle of 60°.

Results and Discussion

Figure 1 shows the ARUPS spectra for the various Pn/metal interfaces as functions of (a) the takeoff angle or (b) the azimuthal angle. For the disordered Pn/Au(111) interface (a1), the Pn-induced peak appears at E_b of 0.96 eV with the linewidth of 0.5 eV, which is slightly broader than that for the Pn/graphite interface of 0.3 eV (not shown), which can be ascribed to the molecular level broadening due to weak O-M interaction [Fig. 1(c1)]. On the other hand, the Pn-induced electronic structure on Cu(111) (a2) is rather different from that on Au(111): the Pn-induced peaks on Cu(111) appear at E_bs of 0.72 and 1.34 eV. These peaks can be ascribed to the molecular levels split due to the hybridization of the molecular orbitals with the substrate wavefunction [Fig. 1(c2)] [1,2], which can modify the energies and orbital symmetries. Such a behavior is observed also for the Pn/Cu(100) (b1) and the Pn/Cu(110) (b2) interfaces. Furthermore, at the single-domain Pn/Cu(110) interface, the resultant split levels show dispersive behavior [2]. This originates from (i) highly ordered film structure and (ii) the intermolecular interaction via the metal substrate due to the hybridization at the interface.

These factors (c1) and (c2) may be dominated by the different O-M bonding distance at the interface, and we consider that the Pn-Cu bonding distance is probably shorter than the Pn-Au bonding distance.

[1] A. Ferretti *et al.*, Phys. Rev. Lett., **99** (2007) 46802.
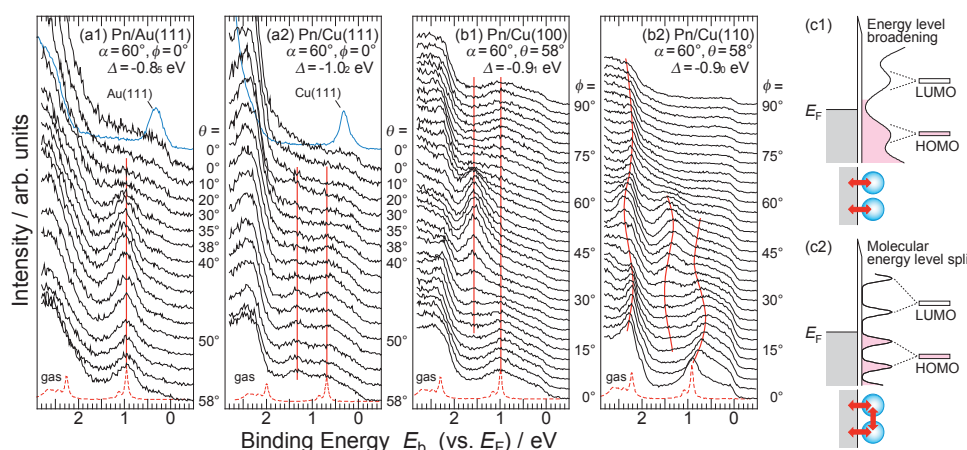[2] H. Yamane *et al.*, Phys. Rev. B, **76** (2007) 165436.

Fig. 1. ARUPS spectra as a function of (a) takeoff angle (θ) and (b) azimuthal angle (ϕ) measured for (a1) the disordered Pn/Au(111) interface, (a2) the disordered Pn/Cu(111) interface, (b1) the multi-domain Pn/Cu(100) interface, and (b2) the single-domain Pn/Cu(110) interface. (c) Possible origins of the interface state: (c1) energy level broadening due to the weak M-O interaction, (c2) energy level splitting due to the hybridization of the molecular orbital with the substrate wavefunction. The vacuum level shift upon adsorption (Δ) is also shown.

Modification of Shockley-Type Surface State and Formation of Charge Transfer State at ZnPc/Cu(111) Interface

H. Yamane[1], K. Kanai[2], Y. Ouchi[1], K. Seki[1]

[1]*Department of Chemistry, Nagoya University, Nagoya 464-8602, Japan*
[2]*Research Center for Materials Science, Nagoya University, Nagoya 464-8602, Japan*

Introduction

The electronic structure at interfaces formed by an organic semiconductor film with a metal electrode is of fundamental importance in discussing the Schottky barrier heights such as the highest-occupied and lowest-unoccupied molecular orbital (HOMO and LUMO) levels at organic-devices interfaces. However, the energetics of organic devices has not yet been understood systematically. To clarify the possibly complicated electrical and structural phenomena at organic/metal interfaces, a more pertinent approach to this issue would be to use a well-characterized system in quantitative electron spectroscopic measurements.

In this work, we studied the electronic structure of thin films of zinc-phthalocyanine (ZnPc), one of the archetypal organic semiconductor, grown on Cu(111) using angle-resolved UV photoemission spectroscopy (ARUPS). We observed the distinctive electronic structure induced by the charge transfer (CT).

Experiment

The ARUPS measurements were performed at the surface temperature of 300 K at the photon energy of 20 eV and the photon incidence angle of 60°.

We obtained a saturated ZnPc monolayer by heating the 5-nm ZnPc film at 700 K; the ARUPS spectra for the heated film shows nearly the same characteristic to that for the 0.3-nm film.

Results and Discussion

Figure 1 shows the film thickness dependence of the ARUPS spectra for the ZnPc/Cu(111) system. In the energy window A, just below the Fermi level (E_F) at around the surface normal ($\theta = 0°$), the Shockley-type surface state of Cu(111) survived even upon formation of the ZnPc monolayer. From the takeoff angle dependence of the ARUPS spectra, we found that the characteristics of the surviving surface state are modified from that of the original one in the peak position at the $\bar{\Gamma}$ point ($0.39 \rightarrow 0.18$ eV), Fermi wavelength k_F ($2.07 \rightarrow 2.23$ nm^{-1}), and the effective mass m^* ($0.42m_0 \rightarrow 1.08m_0$). The adsobate-induced modification of the surface state has been reported for the adsorption of rare gases [1] and a large energy-gap (~ 9 eV) molecule of n-alkane (n-C$_{44}$H$_{90}$) [2]. The observed modification of the surface state upon the ZnPc adsorption, which is slightly different from the previous observations [1,2], may be dominated by the combination of (1) the push back (Pauli repulsion) of the surface electrons and (2) the CT between the molecule and the substrate.

For the 1-ML ZnPc spectra at the surface off-normal ($\theta \geq 38°$), one can see two-prominent peaks labelled B and C in Fig. 1. With increasing the film thickness, peak B shifts gradually to higher binding energy side probably due to the change in (i) the final state screening and (ii) the molecular orientation [3], and the intensity of peak C decreases rapidly. Judging from the thickness dependence of the ARUPS spectra, peak B is ascribed to the (original) HOMO-derived level, and peak C may be ascribed to the CT state.

The formation of the CT state at the ZnPc/Cu(111) interface is unexpected just by considering the ionization energy and the electron affinity of the ZnPc solid and the work function of the Cu(111) substrate of $I_s = 5.2$ eV, $A_s = 3.3$ eV, and $\Phi_m = 4.9$ eV, respectively, which were obtained from our UPS and inverse photoemission spectroscopy experiments (see Fig. 1). For the origin of the CT state, one has to consider (i) the molecular energy level broadening due to organic-metal interaction and (ii) the change in the intermolecular polarization energy due to the presence of the CT-induced dipole. Since the bonding distance at the interface would be a key for further consideration on the interfacial electronic structure of ZnPc/Cu(111), we will perform the X-ray standing wave experiment for the ZnPc/Cu(111) system at ESRF (Grenoble, FRA).
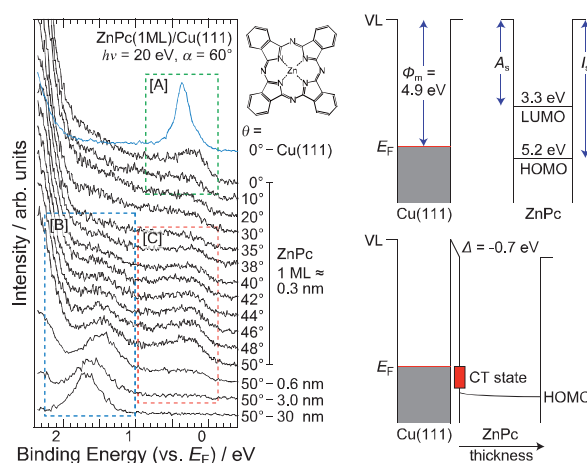

Fig. 1. Film thickness dependence of the ARUPS spectra for the ZnPc/Cu(111) system (left) and the energy level diagrams of the Cu(111) substrate, the ZnPc solid, and the ZnPc/Cu(111) system (right).

[1] F. Reinnert, J. Phys.: Cond. Matter, **15** (2003) S693.
[2] K. Kanai et al., Phys. Rev. B, submitted.
[3] H. Yamane et al., J. Appl. Phys., **99** (2006) 93705.

Asymmetric Synthesis and Decomposition of Amino Acids by Using UVSOR-FEL

K. Kobayashi[1], T. Ogawa[1], S. Shima[1], T. Kaneko[1], H. Mita[2], J. Takahashi[3],
M. Hosaka[4], M. Kato[5]

[1]*Graduate School of Engineering, Yokohama National University, Yokohama 240-8501, Japan*
[2]*Faculty of Engineering, Fukuoka Institute of Technology, Fukuoka 811-0295, Japan*
[2]*NTT Microsystem Integration Laboratory, Atsugi243-0198, Japan*
[3]*Graduate School of Engineering, Nagoya University, Nagoya 464-8601, Japan*
[4]*Masahiro Kato, Institute for Molecular Science, Okazake 444-8585, Japan*

Introduction

The Origin of homochirality of biological molecules such as amino acids has remained one of the most important problems in the field of origins of life and astrobiology. Cronin and Pizzarello reported that some amino acids extracted from carbonaceous chondrites showed significant enantiomeric excesses of L-isomers [1]. Isovaline, a non-proteinous amino acid without a-hydrogen atom, was included in such category of amino acids (Fig. 1). One of the possible scenario for the generation of enantiomeric excesses of amino acids are asymmetric formation or decomposition of amino acids by circular polarized light in space. Bailey found circular polarized light of IR range in space [2]. Takano *et al*. reported that enantiomeric excess of alanine was formed after irradiation of amino acid precursors with UV-CPL [3]. Here we examine decomposition of isovaline by irradiation with UV-CPL from UVSOR-free electron laser (FEL). We also studied possible introduction of chirality to amino acids in thin films by UV-CPL irradiation.
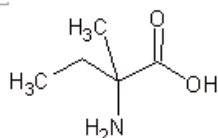
Fig. 1. Isovaline

Experimental

Aqueous solution of isovaline in a quartz cell was irradiated with UV-CPL (Fig. 2): After either R- or L-UV-CPL (wavelength: 216-230 nm) was irradiated, amino acids and amines in resulting products were analyzed by cation-exchange HPLC (Shimadzu LC-10A), and carboxylic acids were determined by capillary electrophoresis (Photal CAPI-3300). D/L ratio of amino acids was measured by reversed-phase HPLC after AQC derivatization (Tosoh DP-8020).

Isovaline aqueous solution was also irradiated with high-energy heavy ions (290 MeV/u carbon ions from HIMAC, NIRS, Japan) or X-rays (6 keV, 27B line of Photon Factory, KEK, Japan).

Thin film of phenylalanine was made by vacuum deposition on an MgF_2 substrate. The film was irradiated with D- or L-CPL. CD spectra were measured after irradiation.
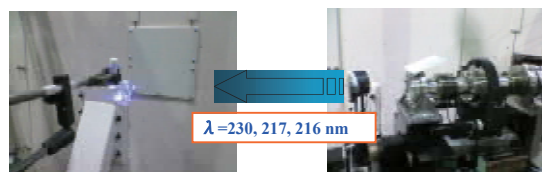

λ =230, 217, 216 nm

Fig. 2. UV-CPL irradiation of isovaline solution

A gaseous mixture of carbon monoxide, ammonia and water was also irradiated with UV-CPL to examine possible formation of amino acid precursors. The resulting product was acid-hydrolyzed, and amino acids were determined by HPLC (Shimadzu LC-10A).

Results and Discussion

When isovaline solution was irradiated with UV-CPL, isovaline was decomposed: Alanine was found as predominant amino acid products, and 2-butylamine and isovaleric acid were also detected. The release of methyl group, carboxylic group, or amino group from isovaline was specific to UV irradiation, since X-rays or heavy ions irradiation of isovaline solution did not give them as major products. Enantiomeric excesses of isovaline or alanine were not detected in the present experiments. As pH of the solution might be important for asymmetric decomposition, we plan to irradiate isovaline solution in acidic/basic conditions.

When phenylalanine thin films were irradiated L- or R-CPL, the resulting films showed apparent CD spectra at 200 nm and 220 nm. They seem to correspond to π-π* and n-π* transitions, individually. It was proved that CPL irradiation introduced chirality to thin film of aromatic amino acids.

Amino acids were formed by UV-CPL irradiation of the gas mixture: Glycine was predominant, followed by alanine. G-value of glycine was 0.0012, which was smaller than that by proton irradiation or that with UV light from D_2 lamp.

[1] J. R. Cronin, S. Pizzarello, Science **275** (1997) 951.
[2] J. A. Bailey *et al*., Science **281** (1998) 672.
[3] Y. Takano *et al.*, Earth Planet. Sci. Lett. **254** (2007) 106.